Modeling and Simulation of a Doubly Fed Induction Generator Based Wind Turbine

Received: 8 June 2022; Revised: 11 August 2022;
Accepted: 25 December 2022
Research Article

Khalid Waleed Nasser
Department of electrical engineering
University of Misan
Misan, Iraq
khalid.waleed@uomisan.edu.iq
ORCID: 0000-0002-2384-7031

***Abstract*— Wind power's fundamental difficulties are becoming more visible as the system's penetration grows. Wind energy fluctuation must be reduced, and large-scale units must be connected to the grid constantly and dependably. Despite conventional power vector control can achieve decoupling control, DFIG has a high reliance on elements; therefore power control and maximum power tracing is a critical area of research. The DFIG model is constructed on the MATLAB/Simulink platform and is based on an examination of active power research's current state. The impact of wind speed on power generated, pitch angle, and reactive power is investigated by simulating the dynamic model of a DFIG WT.**

Keywords—DFIG, wind turbine, doubly fed induction generator,

I. INTRODUCTION

The environment is concerned about the global energy crisis and climate change. Renewable sources of energy have developed as a new model for meeting our society's energy needs. Hydroelectric power, solar, wind, geothermal heat, tides, seas, and biofuel energy supplies have all attracted much attention in recent years. The future of the power sector will be characterized by wind energy. Wind power generation technologies have attracted widespread attention due to their fast development . DFIGs have several advantages in modern energy systems, including operation at varied speeds and real and reactive power characteristics. The stator is connected to the electricity grid directly in DFIG. In contrast, the rotor is connected via a bi-directional converter to regulate active and reactive power among the stator and the alternative current system [1]. The rotor flow is based on wind turbine technology and disconcerts the vector control approach into active and reactive power elements. Rotor current control systems regulate these elements by rectifying the rotor current excitation voltage [2, 3]. The issues should be overcome for massive wind farm operations. The electromechanical model created a nonlinear feedback controller by coupling DFIG with turbines for wind. The increased utilized of replenishable energy is mandated on a global scale owing to traditional power plants' energy key pollution and non-sustainability [4]. Many technical problems involving systems of electricity, such as voltage stability, reliability, and protection. Wind energy is gaining popularity as a sustainable energy source that is less expensive than traditional electricity sources. Wind energy is erratic due to substantial changes in the natural wind. Due to considerable insignificant changes compared to conventional energy sources, the wind energy conversion system confronts major hurdles [5]. The power outage variation generates variation in frequency, implying the unsteadiness of a high penetration system. Because of the large variability in output power, wind energy conversion devices are considered hazardous loads [6]. The transmission of nonlinearity of wind farms owing to the DFIG physical model is affected by wind swiftness and rotation of electro-magnetic torque. For both stator and rotor current flow are nonlinear functions. The rotor current controller must be carefully tuned to maintain the steadiness of the closed-loop technique and adequate transient reaction into the working scope [7, 8]. As well, vector control demands flux prediction or mensuration. It is essential to move up and down to generate units to satisfy active and reactive power requirements [3]. The accompanying preservation expense of such manipulation activities ought kept low, as must the network's requirement for wind turbines to ride through the ability of external AC disruption. An enhanced control in the presence of an imbalanced voltage and enhances the fluctuation in grid voltage is suggested for controlling the overcurrent of the generator by keeping an eye on the network failure [9]. The investigation of the fault current characteristics of DFIGs is a prerequisite for fixing the difficulties of relaying electrical system's protection with DFIGs. These criteria vary from those of a traditional synchronous generator. Under different settings, the fault current properties of DFIG (damping temporal constants as well as transient elements) are variable. As a result, the research of DFIG features for specific situations is required [2, 10-12]. For fault circumstances, numerous research has been recommended. However, due to the intricate consequences of the dynamic reaction of an AC/DC/AC converter according to fault situations, analyzing the current fault characteristics of the DFIG is hugely challenging. The DFIG fault current was investigated on the assumption that the excitation current would be fixed before and after the fault occurred [11-14]. The research is unsuitable for practical systems because it is based on the stated assumption. As other high-quality, research was conducted for properties of fault current while taking in consideration the rotor side converter (RSC) and grid side converter's dynamic response (GSC). The work offered in that study is insufficient to fulfill the criteria of the relaying protection study. To close this gap, a theoretical, analytical approach for the DFIG The characteristic of fault current in non-severe conditions is proposed. The rotor windings are still excited, and the dynamic reaction significantly impacts

the stator fault current characteristics. Wind turbines must be integrated and participate actively in maintaining system stability during and after disruptions or failures. Other system dynamics could deteriorate as a result of this strategy. In the sector of transient investigations, the disruption of the field is separated from the turbine generator's way of behaving [8, 15]. The boundary of the rotor side converter can raise the stator fault current and DC link voltage to achieve the DFIG needs through the voltage dip. The theoretical underpinning of the inquiry was conducted, and the DFIG transient behavior enhanced after the disturbance in the study was removed. The dynamic model analysis was employed in the nonlinear control architecture to settle the nature of the instability and enhance the generator's performance [16].

II. Literature Survey

H. Abouobaida: A control method for a grid connected (DFIG)-based WECS is presented in this research. Control algorithms for the DFIG's grid and rotor side converters, as well as simulation techniques of the design, are described. The established methodology control is simulated in MATLAB-SIMULINK, with the findings given at the conclusion of this study [1]. Adavipalli Chandanaet al., In relation to other renewable energy sources, wind turbines are more expensive. DFIG with Fuel Cells could be used to keep the active power at a consistent level. The power transfer matrix is a fresh idea for governing the DFIG introduced in this study. A matrix converter mechanism-based power/current controller is designed with the goal of protecting the DFIG during malfunctioning situations [4]. NihelKhemiri et al, The design and control concepts for a variable-speed constant-frequency WECS using a (DFIG) are discussed in this research paper. The wind energy converter system performed well under common wind variations, according to simulation findings generated with Matlab/Simulink. A backstepping control scheme is first constructed for the rotor side converter. A backstepping control system was originally created for the (RSC).The GSC is controlled using the same principles [17]. HU Jia-bing et al., A proportional-resonant (P-R) current control scheme and suitable control strategies for (GSC and RSC) are investigated for better control and fully operational of WECS that rely on DFIGs during voltage profile unbalancing circumstances. A P-R current control technique that is applied in the two-phase stator stationary reference for the DFIG's RSC when the system voltage is mismatched was introduced in this academic research with the goal of concurrently controlling the positive and negative sequence rotor currents using no sequential-decomposition method. Baseline calculations of positive and negative sequence rotor currents were shortened according to distinct enhanced control aims based on the positive-sequence d+-axis line voltage direction. The P-R current controller's feasibility was validated by developing and building the appropriate control method for a DFIG wind power generating system under network instability. The results show that the recently developed P-R current controller can execute the RSC's control aims with an exceptional transient response. As a result, the DFIG wind generating system's ride-through capabilities have increased during unbalanced network fault conditions [18]. Jiabing Hu et al., The electromagnetic stability issues with grid-connected DFIG systems are frequently overlooked. This research offers a reduced-order small-signal model that may be used to examine the stability of DFIG's dc-link voltage controller, especially when the ac grid is not performing well. The DFIG flux and quick current control characteristics are ignored in this model. However, the effects of operating points, grid strength, and control loop interactions just on dynamic system performance are considered. A comparison of eigenvalues shows that the suggested model demonstrates the dominant oscillation mode indicated by the detailed model, which is suitable for the stability study of the DFIG's dc-link voltage management system. Control loop interactions are also depicted using influence coefficients. The recently launched model's application studies reveal that it is useful for demonstrating the effect of grid strength on the dynamic response of the DFIGs dc-link voltage controller. At the same moment, the effects of active power control (APC)/reactive power controls (RPC) on phase-locked loop (PLL) and rotor-side converter (RSC) stability of the system are explored [19]. P.GAYATHRI et al., The use of fuel has increased in tandem with the rise in worldwide power demand, harming the environment, and inspiring the use of renewable energy supplies. The wind energy system is the most widely used and meets all power requirements. The DFIG is used in the proposed system for wind energy conversion, as well as harmonics scaling down and frequency management. When two back-to-back coupled Voltage Source Converters (VSCs) are retained between the rotor and the grid in DFIG, the stator is directly connected to the grid. Since the suggested DFIG operates as an active filter and generates active power in the same way as a typical DFIG, nonlinear loads are connected at PCC. The PCC voltage is distorted due to harmonics created by the nonlinear load connected at the PCC. GSC control improves the nonlinear load harmonic currents to the point where the stator and grid currents are harmonic-free. Using a voltage-oriented reference frame, RSC is adjusted to achieve MPPT and also to achieve unity power factor at the stator side. For GSC control, a synchronous reference frame (SRF) control method is used to extract the basic component of load currents. Furthermore, PLL is used to monitor and modulate frequency. The MATLAB Simulink software is used to evaluate this newly presented technology.

III. Generating System in General

Figure 1 shows a structured methodology for generating electrical energy from wind power using a doubly-fed induction generator. The stator is fed to the network straight, whereas the rotor is plugged via a back-to-back converter [15]. The grid side converter is a PWM inverter, whereas the rotor side converter is a current regulate-voltage source inverter [20].

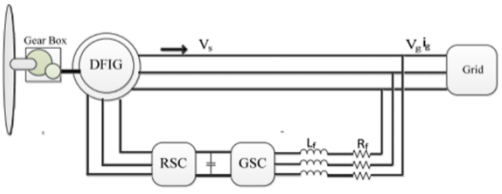

Fig. 1. Wind energy schematic diagram based on the DFIG system

A. Wind Turbine Pattern

The mechanical power caught by a wind turbine is as described in the following:

$$P_m = \frac{1}{2} C_p(\lambda, \beta) \rho R_T^2 \pi v V_\omega^3 \quad (1)$$

Where ρ reflects the density of the air, R_T the wind turbine radius, V_ω the wind speed, and C_p the wind turbine power coefficient. The C_p is calculated by:

$$C_p(\lambda, \beta) = 0.22\left(\frac{116}{\lambda_i} - 0.4\,\beta\text{-}5\right) e^{\frac{-12.5}{\lambda_i}} \quad (2)$$

$$\frac{1}{\lambda_i} = \frac{1}{\lambda + 0.08\,\beta} - \frac{0.035}{\beta^3 + 1} \quad (3)$$

where β symbolizes the blade pitch angle and λ symbolizes the tip speed ratio as described [10].

$$\lambda_{opt} = \frac{\omega_r R_T}{V_\omega} \quad (4)$$

Because of the existence of a gearbox with the gear ratio, the dynamic model wind turbine rotational speed ω_{rot} is related with the rotor speed ω_r:

$$\omega_r = n_g \lambda_{opt} \quad (5)$$

The exact dynamic model of the torque equation of the generator is given by,

$$T_m = \frac{P_m}{\omega_r} \quad (6)$$

It is a proportion of wind turbines that is measured, where Tm represents rotor torque and ωr denotes wind turbine velocity. Wind turbine speed affects the power coefficient. The theoretical maximum Cp is 0.59, although the actual range is 0.2-0.4 [21]. (4) and (5) yield the ideal generator speed for the optimum tip speed ratio:

$${\omega_r}^{opt} = \frac{\lambda_{opt}\, n_g}{R_T} V_\omega \quad (7)$$

This refers to a high level of wind energy extraction P_m^{max} at the moment, the rotor torque of the generator can be calculated as:

$${T_m}^{opt} = \frac{1}{2} \frac{\rho\, \pi\, R_T^5\, C_P^{opt}}{\lambda_{opt}^3} {\omega_r}^{opt} \quad (8)$$

The external input of the mechanical elements of the system is a wind turbine that rotates at the optimum rotational velocity and with the optimum torque of the nonlinear dynamic model of the doubly-fed induction generator.

B. The DFIG Model

The controller is often specified in a synchronous *d-q* frame that is linked to the stator voltage or flux [12, 22]. The generator dynamic model stated in a synchronously rotating frame *d-q* for the suggested control approach is:

$$\begin{aligned} V_{sd} &= R_s I_{sd} + \frac{d\emptyset_{sd}}{dt} - \omega_s . I_{sq} \\ V_{sq} &= R_s I_{sq} + \frac{d\emptyset_{sq}}{dt} - \omega_s . I_{sd} \\ V_{rd} &= R_r I_{rd} + \frac{d\emptyset_{rd}}{dt} - \omega_r . I_{rq} \\ V_{rq} &= R_r I_{rq} + \frac{d\emptyset_{rq}}{dt} - \omega_r . I_{rd} \end{aligned} \quad (9)$$

$$T_{em} = P\, M\, (I_{rd}\, I_{sq} - I_{rq}\, I_{sd}) \quad (10)$$

$$\begin{aligned} \emptyset_{sd} &= L_S\, I_{sd} + m . L_m\, I_{rd} \\ \emptyset_{sq} &= L_S\, I_{sq} + m . L_m\, I_{rq} \\ \emptyset_{rd} &= L_r\, I_{rd} + m . L_m\, I_{sd} \\ \emptyset_{rq} &= L_r\, I_{rq} + m . L_m\, I_{sq} \end{aligned} \quad (11)$$

Where V is the voltage, I is the current, $\emptyset$ is the flux, R is the resistance, L is the inductance, M is the mutual inductance, Tem is the electromagnetic torque, and P is the pole pair number. The following simplified model is adopted for the DFIG wind turbine:

$$\mathrm{J}\frac{\mathrm{d}\omega}{\mathrm{dt}} = \mathrm{T_m} - \mathrm{T_{em}} - \mathrm{K}.\omega \quad (12)$$

where $\mathrm{T_{em}}$ is the generator electromagnetic torque, J is the turbine total inertia, and K is the turbine total external damping. The stator and rotor powers, both real and reactive, are described by:

$$\begin{aligned} \mathrm{P_s} &= V_{sd}\, I_{sd} + V_{sq}\, I_{sq} \\ \mathrm{Q_s} &= V_{sq}\, I_{sd} - V_{sd}\, I_{sq} \\ \mathrm{P_r} &= V_{rd}\, I_{rd} + V_{rq}\, I_{rq} \\ \mathrm{Q_r} &= V_{rq}\, I_{rd} - V_{rq}\, I_{rq} \end{aligned} \quad (13)$$

Turbine speed is regulated as a function of wind speed to increase output power and increase system efficiency. Beyond a large power range, performance at maximum power could be accomplished. Common output power-speed lines as a result of turbine and wind speed are shown in Fig. 2 [5, 21].

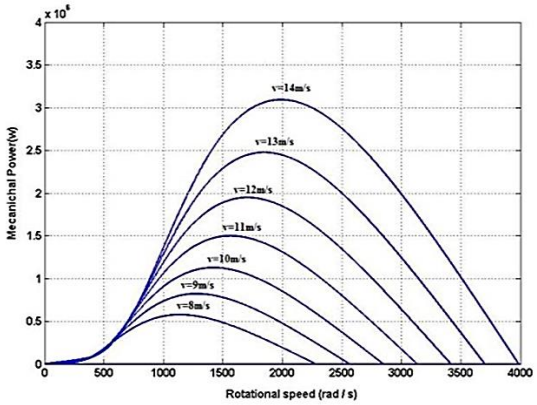

Fig. 2. Electrical output power as a function of turbine speed. Parameter curves are plotted for different wind speeds

C. Modeling of GSC and Grid

As shown in Fig. 3, this section focuses on the design of the AC/DC converter connected to the electrical grid through the RL filter.

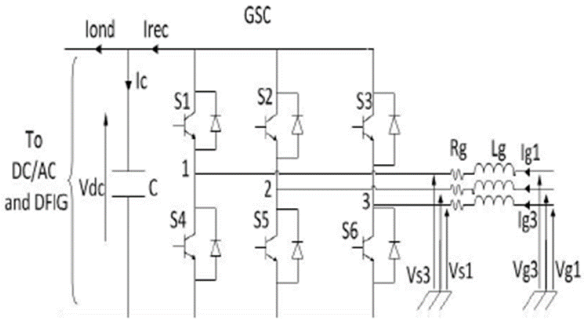

Fig. 3. Grid connected to AC/DC converter

The following equations represent the three-phase grid linked AC/DC converter design:

$$\begin{cases} \frac{CdVdc}{dt} = \text{Irec} - \text{Iond} \\ Vs1 = Vg1 - Rg \cdot Ig1 - Lg \cdot \frac{dIg\ 1}{dt} \\ Vs2 = Vg2 - Rg \cdot \text{Ig}\ 2 - Lg \cdot \frac{dIg\ 2}{dt} \\ Vs3 = Vg3 - Rg \cdot Ig3 - Lg \cdot \frac{dIg3}{dt} \end{cases} \quad (11)$$

With Vgi: electrical network voltages, Igi: electrical network currents, Irec, Iond: AC/DC converter output current and DC/AC converter input current, respectively. Vdc, Ic: the DC connection capacitor's voltage and current, respectively. Vsi: the AC/DC converter's input voltages IGBT transistor (Si).Control Methodology

Figure 4 depicts the controller's structure. It is based on a three-phase model of the wind system's electromechanical conversion chain [6]. Three goals guide the control method:

- "MPPT" is used to control the harvesting of peak wind power (Maximum PowerPoint Tracking),
- Controlling the RSC by adjusting the DFIG stator's electromagnetic torque and reactive power
- Controlling the DC bus voltage, active and reactive power shared with the network to regulate the GSC.

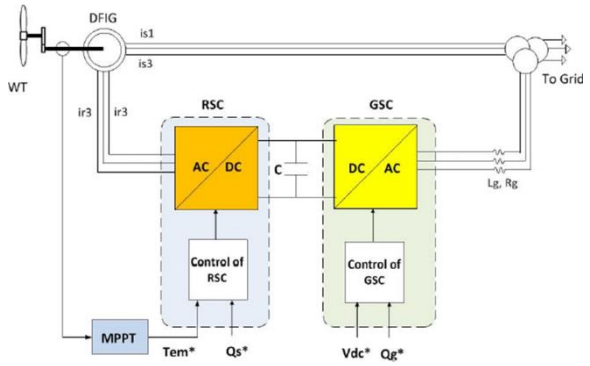

Fig. 4. Control strategy of wind energy conversion system

MPPT technique: Figure 5 illustrates the MPPT control theory for a wind turbine without controlling the rotation speed [12]. The control goal is to maximize wind energy harvesting by tracking the appropriate torque. *Tem**.

$$T_{em} *= k \cdot \omega_m^2 \quad (12)$$

With $$k = \frac{1}{2} \cdot \pi \cdot \rho \cdot R^5 \cdot \frac{Cp_{max}}{\lambda_{opt}^3}$$

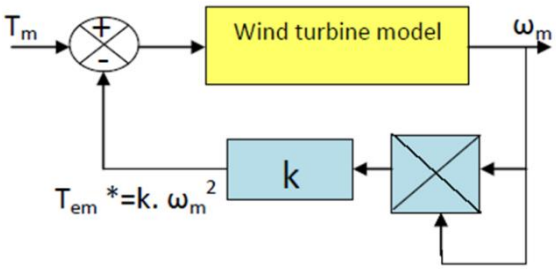

Fig. 5. MPPT control strategy

By adjusting the DFIG's dq-axes rotor currents, the electromagnetic torque and stator reactive power could be controlled. The stator field rotates at synchronous speed in a steady state. The stator flux vector represents this field and provides a visual representation of the phase and flux magnitude. We could construct by selecting the two-phase dq for the rotating stator field and positioning the stator flux vector on the d-axis. [14]:

$$\begin{cases} \Phi_S d = \Phi_S \\ \Phi_{sq} = 0 \end{cases} \quad (13)$$

By examining the selection of reference related to dq rotating stator field and eliminating the resistance of the stator windings, a modification of the DFIG formulas in the dq reference could be derived (9-11):

$$\begin{cases} V_{sq} = \omega_s \Phi_{sd}; V_{sd} = 0 \\ V_{rd} = R_r I_{rd} + \frac{d\Phi_{rd}}{dt} - \omega_r I_{rq} \\ V_{rq} = R_r I_{rq} + \frac{d\Phi_{rq}}{dt} + \omega_r I_{rd} \end{cases} \quad (14)$$

From the (9-11) of the stator and rotor flux in dq axes, the stator currents can be obtained from the following expressions:

$$\begin{cases} I_{sd} = \frac{\Phi_{sd} - m \cdot L_m \cdot I_{rd}}{L_s} \\ I_{sq} = \frac{m \cdot L_m}{L_s} \cdot I_{rq} \end{cases} \quad (15)$$

These expressions are then substituted into the (9-11) of the rotor flux which then become:

$$\begin{cases} \Phi_{rd} = \left(L_r - \frac{(m \cdot L_m)^2)}{L_s} \right) \cdot I_{rd} + \frac{m \cdot L_m}{L_s} \cdot \Phi_{sd} \\ \Phi_{rq} = L_r \cdot I_{rq} - \frac{(m \cdot L_m)^2}{L_s} I_{rq} = L_r \cdot \sigma \cdot I_{rq} \end{cases} \quad (16)$$

With :

$$\sigma = 1 - \frac{(m \cdot Lm)^2}{L_s L_r}$$

is the dispersion coefficient of the DFIG. By replacing the expressions of direct and quadrature components of rotor flux (12) in (14), we obtain:

$$\begin{cases} V_{rd} = R_r I_{rd} + Lr \cdot \sigma \cdot \frac{dI_{rd}}{dt} + e_{rd} \\ V_{rq} = R_r I_{rq} + Lr \cdot \sigma \cdot \frac{dI_{rq}}{dt} + e_{rq} + e_\Phi \end{cases} \quad (17)$$

Where:

$$\begin{cases} e_{rd} = -\sigma \cdot L_r \cdot \omega_r \cdot I_{rq} \\ e_{rq} = -\sigma \cdot L_r \cdot \omega_r \cdot I_{rd} \\ e_{\Phi} = \omega_r \cdot \dfrac{m \cdot L_m}{L_s} \cdot \Phi_{sd} \end{cases} \quad (18)$$

The electromagnetic torque Tem can be expressed from the flux and the stator currents by:

$$T_{em} = P \cdot \left(\Phi_{sd} \cdot I_{sq} - \Phi_{sq} \cdot I_{sd}\right) \quad (19)$$

It can also be expressed in terms of the rotor currents and stator flux:

$$T_{em} = P \cdot \frac{m \cdot L_m}{L_s}\left(\Phi_{sq} \cdot I_{rd} - \Phi_{sd} \cdot I_{rq}\right) \quad (20)$$

From (13), the electromagnetic torque becomes:

$$T_{em} = -P \cdot \frac{m \cdot L_m}{L_s} \cdot \Phi_{sd} \cdot I_{rq} \quad (21)$$

The active and reactive stator powers are expressed by:

$$\begin{cases} P_s = -V_{sq} \cdot \dfrac{m \cdot L_m}{L_s} \cdot \Phi_{sd} \cdot I_{rq} \\ Q_s = V_{sq} \cdot \dfrac{V_{sq} \cdot \Phi_{sd}}{L_s} - \dfrac{m \cdot L_m}{L_s} \cdot V_{sq} I_{rd} \end{cases} \quad (22)$$

Expressions (21) and (22) show that The use of dq reference makes the electromagnetic force created by the DFIG, and thus the stator power, proportional to the q-axis rotor current in the scenario where the stator flux sq is held constant (this criterion is fulfilled in the situation of a stable network connected to the stator of the DFIG). Due to the network's constant, reactive stator power is not proportional to d-axis rotor current. As a result, the reactive stator power can be freely adjusted [23].

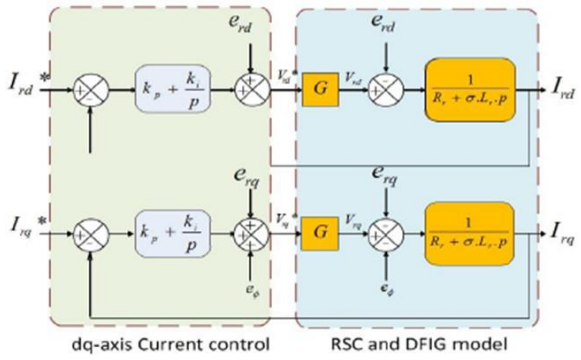

Fig. 6. rotor current regulation on the dq-axis

Assuming that the effect of couplings can be managed of each current separately, the DFIG model in dq reference connected to stator rotating field demonstrates that we may create a rotor currents control. The q-axis rotor current and the d-axis rotor current will be used as reference values for these regulators. To build rotor current control loops, we suppose that the RSC (rotor side converter) is optimal (which correlates to disregarding the wasted time enforced by the power switch drivers) and that the DC/AC converter (RSC) could be described by a gain G which equation is:

$$G = \frac{V_{dc}}{2 \cdot V_p} \quad (23)$$

with: Vp: the magnitude of the triangular carrier of the generation of the PWM. Vdc : voltage of the DC link capacitor. We also suppose that the rotor voltages are the same as their references. Vrk* (k Є [2, 5-12, 15, 20, 22-27]), which means that the magnitude Vp of the carrier should be secured to Vdc / 2, implying a gain G = 1. The block control loops of the dq axes rotor currents diagram is shown in Fig. 6. The controllers used are PI correctors. The reference of the q-axis rotor current is formed from the MPPT control via reference of electromagnetic torque (21 and 12).

The regulation of the stator reactive power provides the reference current for the d-axis rotor current. The RSC's control block diagram is shown in Figure 7. This method can individually control the dq axis rotor currents, as well as the stator's active and reactive power.

The stator flux must be estimated along the d-axis in order to create the rotor's reference current. The grid is assumed to be stable in our study, and the dq reference choice is connected to the rotational field of the stator. Thus, measurements of the d-axis stator and rotor currents in open loop can be used to determine the d-axis stator flux:

$$\Phi_{sd-est} = L_s I_{sd} + m \cdot L_m \cdot I_{rd} \quad (24)$$

After estimating the stator flux, the dq-axes rotor reference currents must be generated. According to (21), the electromagnetic torque is related to the q-axis rotor current, thus we can construct a relationship between the irq* current and the electromagnetic torque *Tem** from block MPPT control by:

$$I_{rq} *= \frac{L_s}{\text{P.m.L } \Phi_{\text{sd\_est}}} \cdot T_{em} \quad (25)$$

Two approaches for rotor d-axis current reference have been developed in the literature:

- The reactive stator power is controlled by this current.
- The purpose of this current is to reduce Joule losses in the rotor and stator.

Since we have opted to control the value of reactive power in this paper, we will stick with the first method.

$$I_{rd} *= \frac{\Phi_{sd-est}}{m \cdot L_m} - \frac{L_s}{m \cdot L_m \cdot V_{sq}} \cdot Q_s * \quad (26)$$

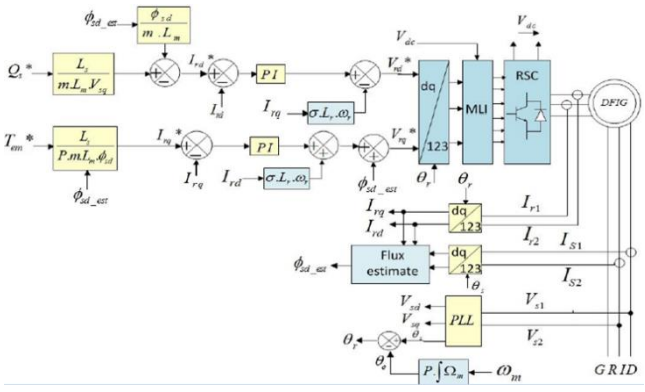

Fig. 7. The Rotor Side Converter's Control Approach (RSC)

Control of the AC/DC converter:

The GSC is an AC/DC converter with an RL filter that connects the DC bus to the electrical network. This converter performs two functions:

- Maintain a steady DC bus voltage independent of the direction and magnitude of the DFIG's rotor power flow.
- Ensure a unity power factor at the point of electrical grid connection.

The instruction of the AC/DC converter is shown in Figure 8. This command carries out the following two tasks:

- Controlling the currents that run through the RL filter
- The DC bus voltage is controlled.

In the dq reference related stator rotating field, (11) becomes:

$$\begin{cases} V_{sd} = V_{gd} - R_g \cdot I_{gd} - L_g \cdot \dfrac{dI_{gd}}{dt} + e_{gd} \\ V_{sq} = V_{sq} - R_g \cdot I_{gq} - L_g \cdot \dfrac{dI_{gq}}{dt} + e_{gq} \end{cases} \quad (27)$$

With

$$\begin{cases} e_{gd=}\omega_s \cdot L_g \cdot I_{gq} \\ e_{gq} = V_{gd} - \omega_s \cdot L_g \cdot I_{gd} \end{cases} \quad (28)$$

Modeling of the AC/DC converter (GSC) connection to the network in the spinning dq stator field reference demonstrates that the current flowing through the RL filter may be changed individually, as can the influence couplings near each axis. These regulators' magnitudes are RL filters in dq axis currents.

In terms of rotor current regulation, the GSC converter model is gain G equal to 1. Figure 9 shows the present technique for block control loops of dq axes. PI controllers are being used. The adjustment terms, dq axis decoupling, and GSC models are shown in these blocks, and they are linked to the network.

The reference dq-axis currents Igd* and Igq* are delivered in the DC bus voltage control and reactive power control blocks at the GSC's grid point of connection, respectively. The below relations describe the active and reactive power exchanged with the electric network:

$$\begin{cases} P_g = V_{gd} \cdot I_{gd} + V_{gq} \cdot I_{gq} \\ Q_g = V_{gq} \cdot I_{gd} - V_{gd} \cdot I_{gq} \end{cases} \quad (29)$$

When losses in the Rg resistance of the RL filter are ignored, and the orientation of the dq reference in relation to the stator rotating field (Vgd = 0) is taken into consideration, the (29) become:

$$\begin{cases} P_g = V_{gq} \cdot I_{gq} \\ Q_g = V_{gq} \cdot I_{gd} \end{cases} \quad (30)$$

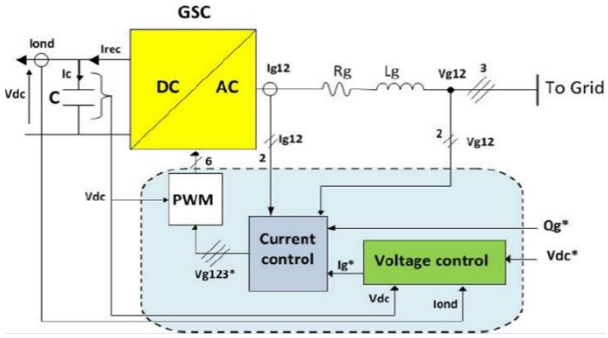

Fig. 8. The Grid Side Converter's command technique (GSC)

From (30), imposing the active and reactive power reference, indicated by Pg* and Qg *, imposing reference currents Igd* and Igq*:

$$\begin{cases} I_{gq} *= \dfrac{P_{g*}}{V_{gq}} \\ I_{gd} *= \dfrac{Q_{g*}}{V_{gq}} \end{cases} \quad (31)$$

The reactive power at the GSC's grid connection point is controlled by the direct current element. The DC bus voltage is regulated by the quadrature component. A null reference of reactive power (Qg * = 0 VAr) can be enforced using this technique.

We can write the DC bus powers using (23):

$$\begin{cases} P_{\text{rec}} = V_{dc} \cdot I_{rec} \\ P_c = V_{dc} \cdot I_c \\ P_{\text{ond}} = V_{dc} \cdot I_{\text{ond}} \end{cases} \quad (32)$$

These powers are linked by the relation:

$$P_{rec} = P_c + P_{\text{ond}} \quad (33)$$

IV. Simulation Results and Discussion

The controller design for a DFIG wind turbine has been implemented utilizing Matlab/Simulink to confirm the robustness of the control strategy and then evaluate the performance of the PI controller execution. Tables II and I present the 1 MW doubly-fed induction generator wind turbine parameters. Fig.3 shows the Turbine Power Characteristics at Pitch angle beta = 0 deg. The DFIG wind turbine controller validates the efficiency of a 1MW wind turbine utilizing Matlab software, which had been run with a 400 V RMS voltage at 50Hz per unit system for the simulation, as shown in Fig.4. At the same time, the Simulink model of the wind turbine is shown in Fig.5. The Controller Rotor Side Converter (RSC) and Grid Side Converter (GSC) are shown in Fig.6. In this situation, wind velocity changes whenever a step-change occurs between 8/s and 12 m/s, as seen in Fig 7. The research proposes a state feedback controller for an accurate DFIG wind generation unit model to improve the machine's grid transient response. The wind turbine system's state variable results are depicted in Fig. 8-Fig. 15. Figs. 8 and 9 show the real and reactive power responses of the DFIG wind generation system. Fig. 10 shows the DC link voltage has been improved for the system.

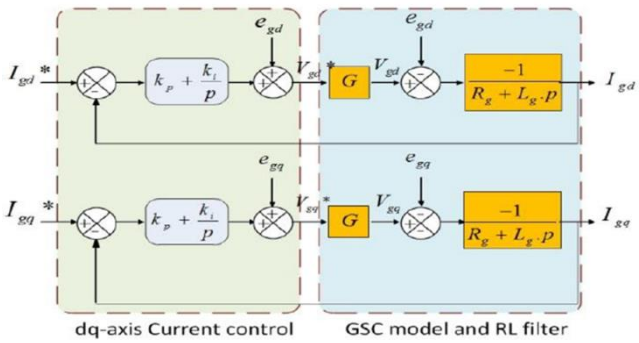

Fig. 9. dq-axis RL filter current control

TABLE I. DFIG PARAMETERS

Parameters	Value	Units
Nominal power	1	MW
Voltage	400	V
Stator resistance	0.00706	PU
Rotor resistance	0.005	PU
Stator self-inductance	0.171	PU
Rotor self-inductance	0.156	PU
Mutual inductance	2.90	PU
Total inertia	5.04	Kg.m^2
Friction Coefficient	0.01	N.mS^{-1}

TABLE II. TURBINE PARAMETERS

Parameters	Value	Unit
Power at point C	0.73	PU/mechanical power
Wind speed at point C	12	m/s

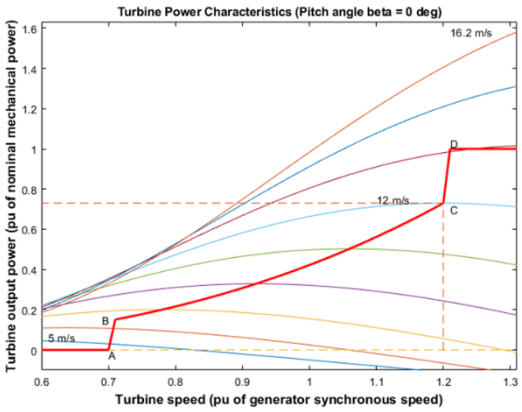

Fig. 10. shows the Turbine Power Characteristics at Pitch angle = 0˚.

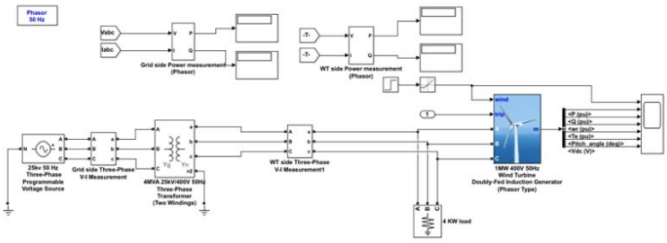

Fig. 11. Simulink model of DFIG wind turbine-load system

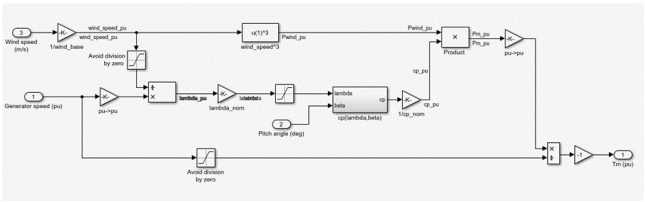

Fig. 12. Simulink model of wind turbine

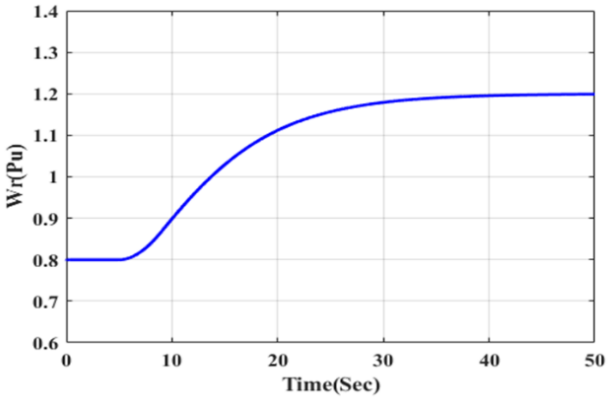

Fig. 13. the Controller Rotor Side Converter (RSC) and Grid Side Converter (GSC)

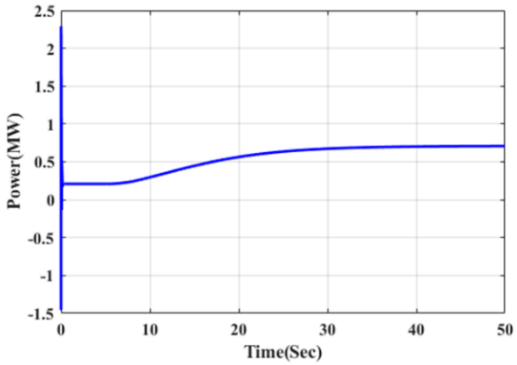

Fig. 14. Step change in Wind speed

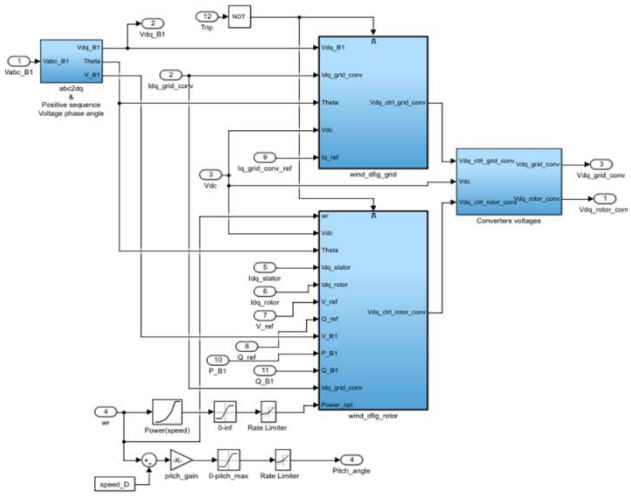

Fig. 15. The real power response of the DFIG wind generation system

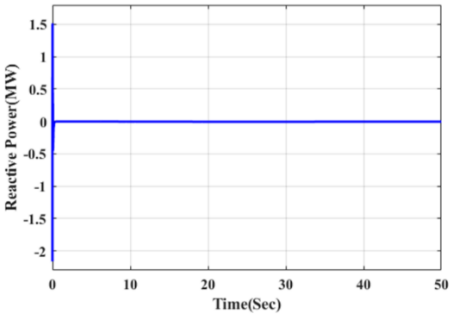

Fig. 16. The reactive power response of the DFIG wind generation system

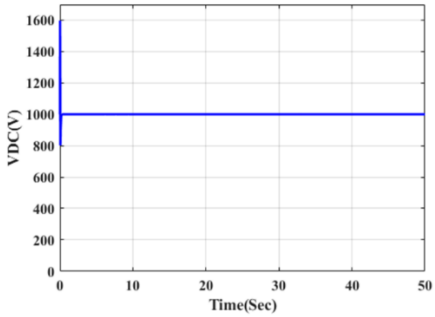

Fig. 17. the DC link voltage

CONCLUSION

The feedback Linearization control approach with a DFIG is developed for the active and reactive power of the wind turbine. It has the potential to increase the wind turbine system's performance dramatically. The DFIG wind turbine was simulated using a wind turbine dynamic model. The results show that sag and overshot of the wind farm's real power and voltage can significantly decrease after the disturbance is eradicated. The damping properties and system stability are improved via feedback approaches. Furthermore, results have been reported on the dynamic response of the system modeling and simulation. It is essential to investigate the analytical features of stability so that the feedback technique used to control the power system can be more successful. Furthermore, the nonlinear dynamic model could be used to create a simple control scheme for the DFIG wind turbine system in the presence of grid voltage disturbances. Finally, to illustrate the feedback technique applications to such a complicated control system, it will be fascinating to analyze the somewhat scenario of a huge energy system analytically.

CONTRUBITION OF THE AUTHORS

The contributions of the authors to the article are equal.

CONFLICT OF INTEREST

There is no conflict of interest between the authors.

STATEMENT OF RESEARCH AND PUBLICATION ETHICS

Research and publication ethics were observed in this study

REFERENCES

[1] H. Abouobaida, "Modeling and Control of Doubly Fed Induction (DFIG) Wind energy conversion system," Journal of Electrical Engineering, vol. 15, no. 1, pp. 12-12, 2015.

[2] S. Ahyaten and J. E. Bahaoui, "Modeling of Wind Turbines Based on DFIG Generator," in Multidisciplinary Digital Publishing Institute Proceedings, 2020, vol. 63, no. 1, p. 16.

[3] D. Chatterjee and Z. H. Rather, "Modelling and Control of DFIG-based Variable Speed Wind Turbine," ed: Indian Academy of Sciences, Bengaluru, India, 2018.

[4] A. Chandana, C. Mutta, and G. V. M. Kiran, "MODELLING AND CONTROLLING OF DFIG BASED WIND SYSTEM USING POWER MATRIX TECHNIQUE," 2018.

[5] Z. Mi, L. Liu, H. Yuan, P. Du, and Y. Wan, "A novel control strategy of DFIG based on the optimization of transfer trajectory at operation points in the islanded power system," Mathematical Problems in Engineering, vol. 2016, 2016.

[6] K. Noussi, A. Abouloifa, H. Katir, and I. Lachkar, "Modeling and control of a wind turbine based on a doubly fed induction generator," in 2019 4th World Conference on Complex Systems (WCCS), 2019: IEEE, pp. 1-5.

[7] B. Qinyu, Y. Lin, M. Jiayi, L. Tianqi, Z. Xiaotian, and W. Youyin, "Study of Double Fed Wind Turbine Modified Simulation Model in Grid Operation," in 2018 China International Conference on Electricity Distribution (CICED), 2018: IEEE, pp. 2023-2028.

[8] R. Rajasekaran and M. Mekala, "Research Issues in DFIG Based Wind Energy System," ELECTRONICS, vol. 22, no. 1, pp. 40-47, 2022.

[9] M. Abulizi, L. Xie, and K. Wang, "Simulation Study of DFIG Wind Turbine under Grid Fault Open-Circuit," in 2019 IEEE 3rd International Conference on Green Energy and Applications (ICGEA), 2019: IEEE, pp. 89-94.

[10] G. S. Kaloi, J. Wang, and M. H. Baloch, "Dynamic modeling and control of DFIG for wind energy conversion system using feedback linearization," Journal of Electrical Engineering and Technology, vol. 11, no. 5, pp. 1137-1146, 2016.

[11] A. G. Abo-Khalil, A. Alghamdi, I. Tlili, and A. M. Eltamaly, "Current controller design for DFIG-based wind turbines using state feedback control," IET Renewable Power Generation, vol. 13, no. 11, pp. 1938-1948, 2019.

[12] A. B. Lajimi, S. A. Gholamian, and M. Shahabi, "Modeling and control of a DFIG-based wind turbine during a grid voltage drop," Engineering, Technology & Applied Science Research, vol. 1, no. 5, pp. 121-125, 2011.

[13] B. Qin, H. Li, X. Zhou, J. Li, and W. Liu, "Low-voltage ride-through techniques in DFIG-based wind turbines: A review," Applied Sciences, vol. 10, no. 6, p. 2154, 2020.

[14] T. M. Masaud and P. Sen, "Modeling and control of doubly fed induction generator for wind power," in 2011 North American Power Symposium, 2011: IEEE, pp. 1-8.

[15] B. Pokharel, Modeling, control and analysis of a doubly fed induction generator based wind turbine system with voltage regulation. Tennessee Technological University, 2011.

[16] D. Li, M. Cai, W. Yang, and J. Wang, "Study of Doubly Fed Induction Generator Wind Turbines for Primary Frequency Control," in 2020 IEEE 4th Conference on Energy Internet and Energy System Integration (EI2): IEEE, pp. 2690-2695.

[17] N. Khemiri and A. Khedher, "A comparison of conventional and modified vector control strategies for controlling transient currents and voltage dips in grid‐connected wind and photovoltaic hybrid system," Environmental Progress & Sustainable Energy, vol. 39, no. 5, p. e13415, 2020.

[18] J. Hu, Y. He, L. Xu, and B. W. Williams, "Improved control of DFIG systems during network unbalance using PI–R current regulators," IEEE Transactions on Industrial Electronics, vol. 56, no. 2, pp. 439-451, 2008.

[19] J. Hu, Y. Huang, D. Wang, H. Yuan, and X. Yuan, "Modeling of grid-connected DFIG-based wind turbines for DC-link voltage stability analysis," IEEE Transactions on Sustainable Energy, vol. 6, no. 4, pp. 1325-1336, 2015.

[20] Z. Dekali, L. Baghli, A. Boumediene, and M. Djemai, "Control of a grid connected DFIG based wind turbine emulator," in 2018 5th International Symposium on Environment-Friendly Energies and Applications (EFEA), 2018: IEEE, pp. 1-6.

[21] G. Abad, J. Lopez, M. Rodriguez, L. Marroyo, and G. Iwanski, Doubly fed induction machine: modeling and control for wind energy generation. John Wiley & Sons, 2011.

[22] M. Nadour, A. Essadki, and T. Nasser, "Coordinated control using backstepping of DFIG-based wind turbine for frequency regulation in high wind energy penetrated system," Mathematical Problems in Engineering, vol. 2020, 2020.

[23] S. Gupta and A. Shukla, "Improved dynamic modelling of DFIG driven wind turbine with algorithm for optimal sharing of reactive power between converters," Sustainable Energy Technologies and Assessments, vol. 51, p. 101961, 2022.